ELSEVIER

Journal of Molecular Catalysis A: Chemical 194 (2003) 153–167

JOURNAL OF MOLECULAR CATALYSIS A: CHEMICAL

www.elsevier.com/locate/molcata

On the acid-dealumination of USY zeolite: a solid state NMR investigation

Zhimin Yan [a], Ding Ma [a], Jianqin Zhuang [a], Xianchun Liu [a], Xiumei Liu [a], Xiuwen Han [a], Xinhe Bao [a,*], Fuxiang Chang [b], Lei Xu [b], Zhongmin Liu [b]

[a] *State Key Laboratory of Catalysis, Dalian Institute of Chemical Physics, Chinese Academy of Sciences, 457 Zhongshan Road, P.O. Box 110, Dalian 116023, PR China*

[b] *Nat. Gas Utilizat. & Appl. Catalysis Lab, Dalian Institute of Chemical Physics, Chinese Academy of Sciences, Dalian 116023, PR China*

Received 26 March 2002; received in revised form 12 July 2002; accepted 20 August 2002

Abstract

The dealumination of USY (ultrastable Y) zeolites by nitric acid and oxalic acid treatment was systematically investigated by multinuclear solid-state NMR and MQ MAS NMR experiments. The results show that both acids are very effective in removing non-framework Al as well as framework Al but that aluminum is extracted from the lattice at a higher rate by oxalic acid even at low concentrations. The presence of different species (e.g. silanol nest, Al–OH, four-coordinated framework Al, six-coordinated framework Al, six-coordinated non-framework Al and five-coordinated non-framework Al) was detected, and their changes were followed during the dealumination. The investigation gives evidence that the breakdown of the parent USY zeolite mainly depends on the degree of dealumination and that non-framework Al exerts a great effect on the acidity of the USY zeolite. Leaching-induced increase in the Brønsted acidity of the USY zeolite was also observed by ^{1}H MAS NMR spectroscopy. The different distribution of Al species in these samples accounted for the different catalytic performance of *n*-dodecane cracking.

Keywords: Y zeolite; Dealumination; Solid-state NMR; MQ MAS NMR; Acidity; Cracking

1. Introduction

It is well known that Y type zeolites of high-silica content cannot be synthesized directly due to the synthesis limits of the Si/Al ratio, i.e. between 2.5 and 2.9. To obtain highly siliceous zeolite Y, it is necessary to have a post-synthesis treatment (dealumination), in which the Al atoms are expelled from the zeolite lattice. As a result non-framework Al species are formed. Dealumination can be accomplished by thermal or hydrothermal treatments, [1] acids leaching, [2] and chemical treatments with hexafluorosilicate or silicon tetrachloride [3–6]. Among these methods, hydrothermal treatment is the most frequently used one, and the resulting material, USY (ultrastable Y) zeolites, being modified in the framework Si/Al ratio, structure and acidity, usually exhibit improved reactivity, selectivity and coking behavior for a catalytic reaction, which is of great interest to the petroleum industry [1,7]. These changes have been attributed to the structural dealumination and the presence of non-framework aluminum [8–10]. It has been suggested that the amount of non-framework Al species, formed during the ultrastabilization, is one of the key factors that influ-

* Corresponding author. Tel.: +86-411-4379116; fax: +86-411-4694447.
E-mail address: xhbao@dicp.ac.cn (X. Bao).

1381-1169/02/$ – see front matter © 2002 Published by Elsevier Science B.V.
PII: S1381-1169(02)00531-9

ences significantly the cracking activity towards hydrocarbons [11]. Meanwhile, the presence of a large amount of non-framework Al has a detrimental effect on the catalytic and transport properties, so that a subsequent acid leaching to extract them is necessary. In addition, chemists have different opinions on the assignment of those non-framework Al species, characterized by a broad ^{27}Al band between the bands of the tetrahedrally-coordinated Al (at ≈60 ppm) and octahedrally-coordinated Al (at ≈0 ppm) in the ^{27}Al NMR spectra of steamed USY [12–28]. It can be visualized that, when a given chemical agent extracts a non-framework Al, the efficiency will be influenced by the degree of polymerization or the local environment of the non-framework Al. As a result, a modification in the distribution of aluminum by acid leaching can be controlled by the type and concentration of the acid used, the temperature employed and the duration of the treatment. The nature and variation of these aluminum species during acid leaching are of great importance for a better understanding of the catalytic behavior of these treated zeolites and, therefore, are worth further studying.

In this work, USY zeolites were modified through different acid dealumination procedures by removing different fractions of framework and/or framework Al atoms. The conditions of dealumination, such as the type of acid, the concentration and the temperature, were varied systematically in order to obtain a regular change of structural and acidic properties of the USY zeolite as well as the Al coordination during the dealumination process. The resulting samples were characterized by XRD and solid state NMR spectroscopy, with XRD measurements for structure breakdown, and NMR measurements for analysis of structure, Al coordination, and acid sites (types, strength, and number of hydroxyl groups in zeolites). The different distribution of Al species in these samples accounted for the different catalytic performance of *n*-dodecane cracking.

2. Experimental

2.1. Acid dealumination

Zeolite NaY (Si/Al = 2.5) was synthesized according to the conventional hydrothermal method. The USY sample was prepared from NH_4-exchanged zeolite Y obtained by three-fold contact of NaY with a saturated aqueous solution of NH_4NO_3 at 353 K, followed by washing with deionized water. After being dried at 373 K, the NH_4–Y sample was then treated at 873 K for 4 h in a 100% steam atmosphere to obtain the USY sample. Subsequently, the USY zeolite was treated with nitric acid or oxalic acid using a proportion of 1 g zeolite per 20 ml solution. The acid treatment was carried out at room temperature or under reflux conditions for 8 h. The concentration of oxalic acid was varied systematically from 0.1 to 1N and that of nitric acid from 0.25 to 1N. The suspension was then washed with deionized water and dried in an oven at 393 K overnight.

The codes of the samples reflect their treatment conditions. The acid and its concentration are given in parentheses. The temperature at which the sample was treated is also given. If the sample was leached by 0.1N oxalic acid at room temperature, it is denoted by USY(0.10)RT, while USY(1N)HT means that the USY was treated with 1N nitric acid under a reflux condition.

2.2. Characterization

2.2.1. XRD measurements

Powder XRD patterns were collected on a D/max-γb type X-ray diffractometer (RIGAKU) using Cu Kα radiation. The scan speed was 5°/min and the scan range was 5–50° 2θ. The crystallinity was determined by using HY zeolite as the reference material and the total intensity of the strongest reflections in the region $15 < 2\theta < 36°$.

2.2.2. NMR Measurements

The NMR spectra were obtained at 9.4 T on a Bruker DRX-400 spectrometer using 4 mm ZrO_2 rotors at room temperature. ^{29}Si MAS NMR spectra with high power proton decoupling were obtained at 79.49 MHz using a pulse of 0.8 μs, a repetition time of 4 s, and 2000 scans. $^{1}H \rightarrow ^{29}$ Si cross-polarization (CP)/MAS NMR experiments [28], which can selectively enhance the signals of Si atoms strongly when interacted with hydroxyl groups, were performed with a 4 s repetition time, 4000 scans and an optimized contact time of 1.5 ms. All ^{29}Si spectra were recorded on samples spun at 4 kHz and referenced to 4,4-dimethyl-4-silapentane sulfonate sodium

(DSS) which has a chemical shift of 0 ppm from TMS.

For the ^{1}H MAS NMR measurements, a home-made and specially-designed apparatus was used to conduct the dehydration of the zeolite, which is described in our previous report [29,30]. After dehydration, the sample can be transferred in situ into the conventional NMR rotor, and sealed without contacting air or moisture. The rotor packed by this method can rotate to the upper speed of 12 kHz, and it is proved by proton NMR experiments that no moisture leakage from the atmosphere can be observed within 2 days. In the present experiment, the samples were evacuated typically under 10^{-2} Pa at 723 K for 20 h. The ^{1}H MAS NMR spectra were collected at 400.1 MHz using single-pulse experiments with 1 μs $\pi/10$ pulse, a 4 s recycle delay, and 200 scans, and with a saturated aqueous solution of DSS (0 ppm from TMS) as a secondary chemical shift reference.

Before the measurement of the ^{27}Al MAS NMR spectra, all samples were fully hydrated in a desiccator with a saturated NH_4NO_3 solution for 48 h to avoid as much as possible detection failures of the Al species due to their asymmetrical environments. The ^{27}Al MAS NMR spectra were recorded at 104.3 MHz (9.4 T) using a 0.75 μs $\pi/12$ pulse with a 3 s recycle delay and 400 scans.

It is well recognized that ^{27}Al NMR spectroscopic methods are very useful in the study of zeolite chemistry, but the sizable second-order quardupolar interaction at Al, which contains higher-ranking anisotropic terms, cannot be completely averaged out by MAS. Methods such as double rotation (DOR) [31], dynamic angle spinning (DAS) [32], multiple-quantum (MQ) MAS [33], and satellite transition (ST) MAS [34] have been proposed to overcome this drawback. Among these, MQ MAS, which was proposed by Frydman and Harwood [33] and Frydman and co-workers [35], appears to be the most promising [36]. ^{27}Al MQ MAS experiments were carried out on a Bruker DRX-400 NMR spectrometer, equipped with a Bruker double-resonance MAS NMR probe with a 4 mm rotor and with the ^{27}Al Larmor frequency of 104.26 MHz. In the experiments, the sample spinning rate was controlled at 10 kHz with a fluctuation of less than ±5 Hz by a Bruker pneumatic MAS unit. In concert with the TPPI technique [37], pure-phase MQ MAS spectra were obtained using a *z*-filter method [38], where the phase cycling was designed to select the coherence pathway of $0 \rightarrow \pm 3 \rightarrow 0 \rightarrow -1$. The first hard pulse was to create the triple-quantum (TQ) coherence, while the second one was to convert the TQ coherence into the zero-quantum (ZQ) coherence. RF amplitude of 100 kHz was used in the experiments for the first and the second pulses and their pulse lengths were optimized to be 4 and 1.8 μs, respectively. The third pulse was used to select the central transition of ^{27}Al. In the experiments, a low RF amplitude of 10 kHz was used for this selective pulse. The spectra were recorded with 512×256 data points and zero-filled to 512×512 before 2D Fourier transform. For each t_1 increment, 48 scans were used to accumulate the signals with a recycle delay of 2 s. A shearing transformation was performed after the 2D transform. The chemical shift was referenced to $[Al(H_2O)_6]^{3+}$ in a 1 M $Al(NO_3)_3$ aqueous solution at 0 ppm.

2.3. Catalytic test

Cracking of *n*-dodecane was carried out in a quartz tubular fixed bed microreactor (6 mm i.d.) at 673 K. Each zeolite was pressed into a large wafer at 20 MPa (2923 psi), then broken into 40/60 mesh pieces. Zeolite of 0.02–0.2 g was mixed with 60/80 mesh quartz chips sufficient to make a total bed volume of 0.35 cm^3 in the flow reactor. The zeolite was sandwiched between two layers of acid washed quartz wool, which resulted in a negligible pressure drop across the reactor. All the catalysts were pre-treated by heating in N_2 flow at 10 K/min to 673 K and holding at 673 K for 0.5 h.

Nitrogen was saturated with *n*-dodecane (Aldrich, 99% purity) at 273 K and passed through the reactor, giving a *n*-dodecane volume feed flow rate of 0.07 cm^3/min. Reaction products were analyzed by an on-line gas chromatograph with a flame ionization detector (FID), and the weight percentage selectivities were calculated assuming an FID response factor of 1.0 for all hydrocarbons [39].

3. Results and discussion

3.1. XRD study

Fig. 1 shows the XRD patterns of USY after different treatments. The powder XRD diffractograms

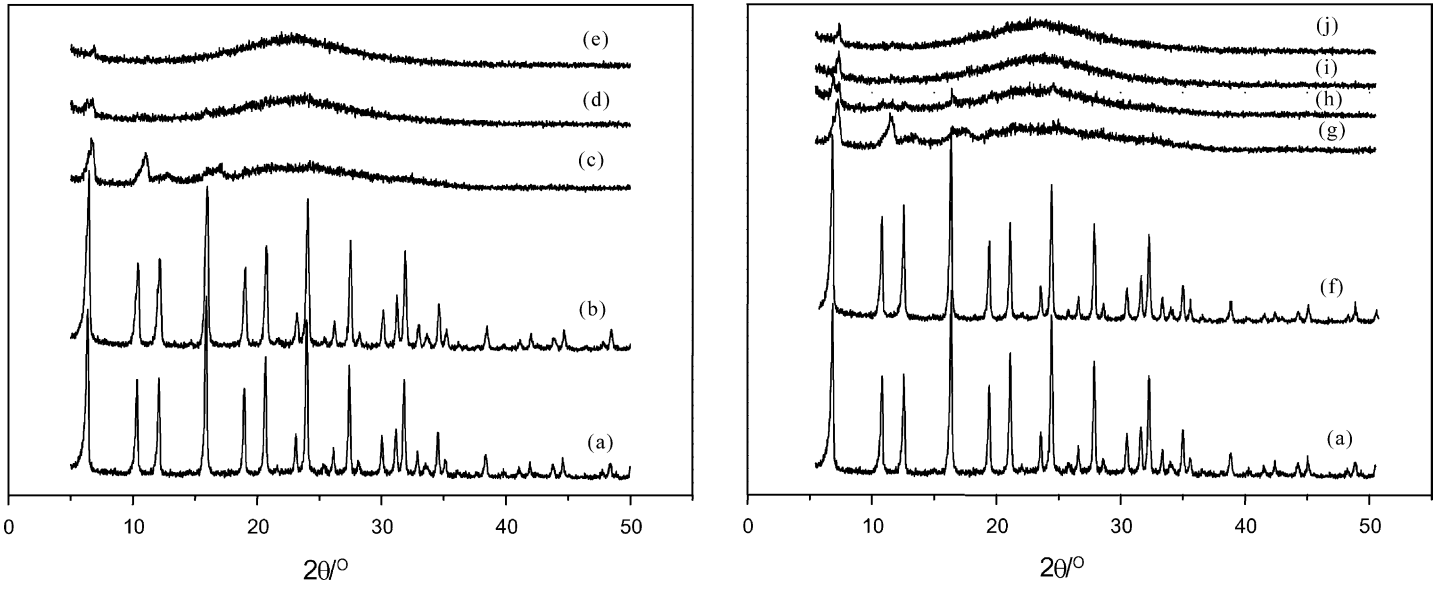

Fig. 1. Powder XRD patterns of USY after nitric acid (left) and oxalic acid (right) treatments. USY (a), USY(0.25N)HT (b), USY(0.5N)RT (c), USY(0.5N)HT (d), USY(1N)HT (e); USY(0.1O)HT (f), USY(0.25O)RT (g), USY(0.25O)HT (h), USY(0.5O)HT (i), USY(1O)HT (j).

show a progressive breakdown of the crystalline structure of the zeolite. The XRD patterns of the USY and USY(0.25N)HT are typical of Y zeolite and indicate a high framework crystallinity. Under more severe leaching conditions (>0.25N nitric acid), the diffraction peaks become weaker and weaker, indicating a collapse of the framework structure, while the broad peak due to the amorphous phase (silica–alumina) becomes more and more obvious. These observations reveal that the formation of the amorphous phase is accompanied with the breakdown of the zeolite framework structure. As for the oxalic acid treatment, the framework breakdown occurs after the leaching by 0.25N oxalic acid at room temperature. Compared with nitric acid, oxalic acid is more effective for the extraction of lattice aluminum. The difference in dealumination behavior can be explained by the dual nature of the oxalic acid, i.e. it acts both as a hydrolysing as well as a chelating agent, forming a trioxalato aluminum complex with a high complexation constant ($\log\beta_3 = 15.1$) [40]. Complexation is the driving force of the observed high aluminum-extraction efficiency of oxalic acid.

3.2. ^{29}Si MAS and CP/MAS NMR

The ^{29}Si MAS NMR spectra of the USY samples are shown in Fig. 2. It is well known that a ^{29}Si MAS NMR spectrum of the Y zeolite may contain up to five lines depending on the number of aluminum atoms and silanol groups connected to the silicon atom [41]. The ^{29}Si MAS NMR spectrum of the parent USY sample (Fig. 2a) shows the presence of four components, corresponding to Si(0Al), Si(1Al), Si(2Al) and Si(3Al) species at −108, −103, −98, and −93 ppm, respectively. After leaching by 0.25N nitric acid under reflux for 8 h, the intensities of these lines are nearly unchanged, which suggests that the framework structure is kept almost intact. However, with the concentration of the nitric acid solution being increased to 0.5N, there is another line developed at −113 ppm, which is assigned to Si(4Si) of silica (as shown in Fig. 2c). Using second ion mass spectroscopy, Dwyer et al. [42] have illustrated that surface layers rich in silica can be produced in Y zeolite after a chemical treatment. At this stage, some of the framework Al species are removed from the lattice by nitric acid and a large part of the framework is ruined, as indicated by its corresponding XRD pattern (Fig. 1c). Meanwhile, it is clear that other bands (those at −108 and −103 ppm) become broadened as compared with the parent USY (Fig. 2a and c), suggesting that acid treatment leads to a distortion of the coordination environment of the corresponding framework silicon atoms and, thus increases the chemical shift distribution. When more severe conditions are used, the intensity of the line at −113 ppm becomes more pronounced, while the characteristic zeolitic band at −108 ppm gradually

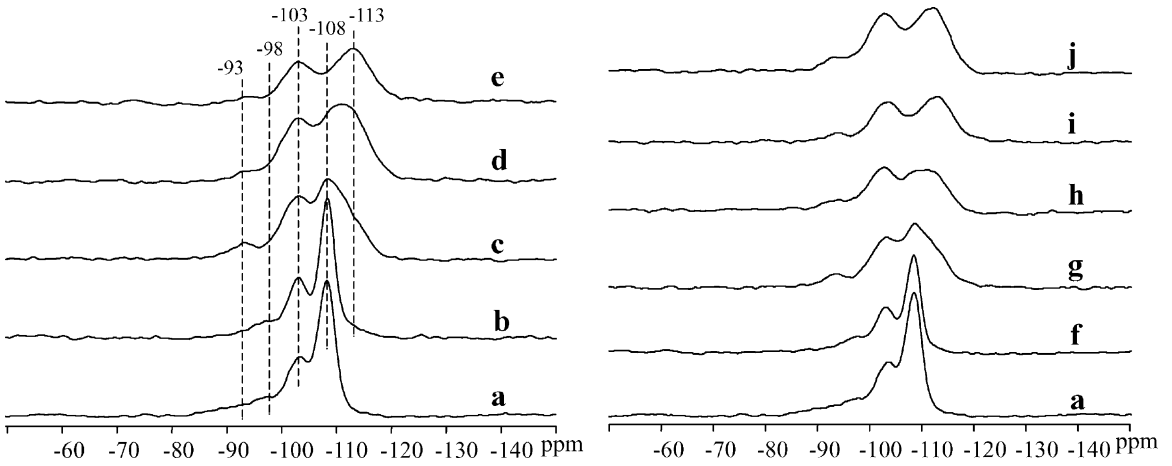

Fig. 2. ^{29}Si MAS NMR spectra of USY after nitric acid (left) and oxalic acid (right) treatments. USY (a), USY(0.25N)HT (b), USY(0.5N)RT (c), USY(0.5N)HT (d), USY(1N)HT (e); USY(0.1O)HT (f), USY(0.25O)RT (g), USY(0.25O)HT (h), USY(0.5O)HT (i), USY(1O)HT (j).

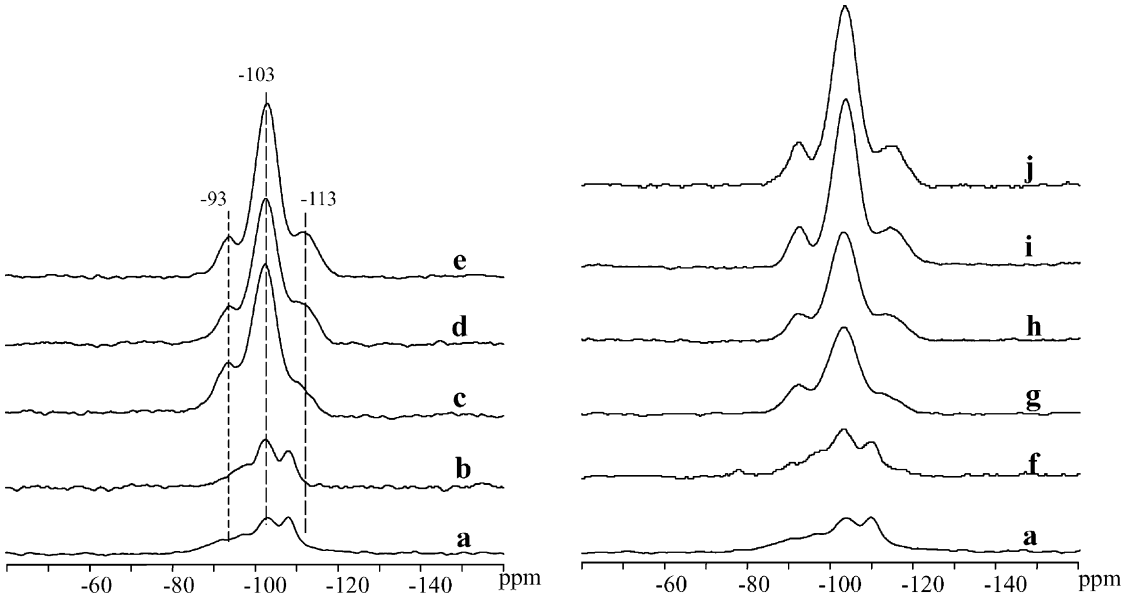

Fig. 3. ^{29}Si CP/MAS NMR spectra of USY after nitric acid (left) and oxalic acid (right) treatments. USY (a), USY(0.25N)HT (b), USY(0.5N)RT (c), USY(0.5N)HT (d), USY(1N)HT (e); USY(0.1O)HT (f), USY(0.25O)RT (g), USY(0.25O)HT (h), USY(0.5O)HT (i), USY(1O)HT (j).

disappears (Fig. 2d and e), showing that the framework of the USY is now almost entirely collapsed, as revealed by its XRD patterns (Fig. 1d and e). If the sample is treated with 1N nitric acid under a reflux condition for 8 h, then the Si(4Si) line and the one at −103 ppm become dominant (Fig. 2e), with a trace amount of species at −93 ppm as a very weak shoulder. It is necessary to make an unambiguous assignment of the peaks at −93 and −103 ppm because, for example, in the case of USY(1N)HT, we can hardly attribute them solely to the Si(3Al) and Si(1Al) species, respectively. In order to get an insight into this problem, the ^{1}H → ^{29}Si CP technique is applied. The corresponding ^{1}H → ^{29}Si CP/MAS NMR spectra of these samples are indicated in Fig. 3. As can be seen, compared with Fig. 2a, the relative ratio of the intensity of the line at −103 ppm to that at −108 ppm increased in the CP spectrum of the USY (as shown in Fig. 3a), suggesting that the line at −103 ppm may be partly due to the $(OSi)_3SiOH$ species that contains a silanol group [41]. Thus, the line at −103 ppm is in fact an overlap of Si(1Al) and $(OSi)_3SiOH$ sites in the spectrum of parent USY. After the leaching by the 0.25N nitric acid, the intensity of the line at −103 ppm is further increased with respect to that of the line at −108 ppm, and attains the maximum. This fact shows that nitric acid can remove lattice aluminum from the zeolite framework, thus resulting in the so-called silanol nests, which is confirmed by the following ^{1}H MAS NMR spectra which show an increase in the intensity of the silanol groups at 1.7 ppm. However, the intensities of the NMR profiles of both the USY and the USY(0.25N)HT are relatively low compared with those of the USY(0.5N)RT, USY(0.5N)HT and USY(1N)HT, indicating that the amount of silanol groups in USY and USY(0.25N)HT is small. The intensity of the line at −103 ppm increases dramatically as the treatment conditions become more severe (as shown in Fig. 3c–e). The enhanced signals at −93 ppm illustrate the presence of the $(SiO)_2Si(OH)_2$, also due to Al removal [41]. Moreover, the peak at −113 ppm corresponding to Si(4Si) of silica becomes more obvious. At the same time, no peak can be detected in the ^{27}Al MAS NMR spectrum of the USY(1N)HT. These results indicate that a large number of the silanol groups are formed and the regular framework structure is lost. For the severely treated samples, the bands at −103 and −93 ppm are mainly attributed to

the $(OSi)_3SiOH$ and $(SiO)_2Si(OH)_2$ species, respectively. The same results have been achieved in the following ^1H MAS NMR experiments.

The ^{29}Si MAS and CP/MAS NMR spectra reveal that framework Al could be dealuminated by acid leaching, while at the same time, the formation of amorphous silica occurs and becomes pronounced as more severe leaching conditions are imposed. The variation in individual peak intensity indicates a progressive dealumination of the USY framework. XRD studies of these same catalysts have also produced results indicative of a progressive dealumination in good qualitative agreement with the ^{29}Si NMR data.

The ^{29}Si MAS and CP/MAS NMR spectra of the USY after oxalic acid treatment are also shown in Figs. 2 and 3. Similar phenomena are observed despite the relatively low concentration of the oxalic acid used.

3.3. ^{27}Al MAS NMR

^{27}Al MAS NMR has been widely used to follow the local Al environment as a function of the treatment. The ^{27}Al MAS NMR spectra of the USY after various treatments are given in Fig. 4. When the ^{27}Al MAS NMR spectrum of the parent USY is analyzed (Fig. 4a), three components are detected centered at 60, 30 and 0 ppm. The two typical signals, namely at 0 and 60 ppm, corresponding to octahedrally and tetrahedrally-coordinated Al species, respectively, can be clearly distinguished. Between them, a broad and tailing band centering around 30 ppm, which is commonly ascribed to five-coordinated Al, is observed. The corresponding acid-leached samples show an apparent decrease in the area of the peak at ca. 30 ppm. For the USY(0.5N)RT and USY(0.5N)HT samples, this peak is virtually absent. At the same time, the peaks at around 60 and 0 ppm undergo different changes. As shown in Fig. 4a and b, both the peaks at 60 and 0 ppm seem to become narrowed upon a 0.25N nitric acid leaching treatment. It is especially the case for the one at 0 ppm. The reason for this observation could be the removal of the superimposed broad peak at ca. 30 ppm, thus leading to a sharpening of these peaks. However, the possibility of the overlap of two resonances at ca. 0 ppm could also account for the observed band narrowing at 0 ppm for the zeolite after acid leaching (as shown in Fig. 4b and e). By means of a high-field NMR instrument (19.6 T), we have recently demonstrated that there are two overlapped octahedral aluminum species around 0 ppm for a dealuminated HMCM-22 zeolite: the narrow one is associated with the zeolite framework while the broad one is non-framework in nature [43]. Here, with acid treatment, the broad one

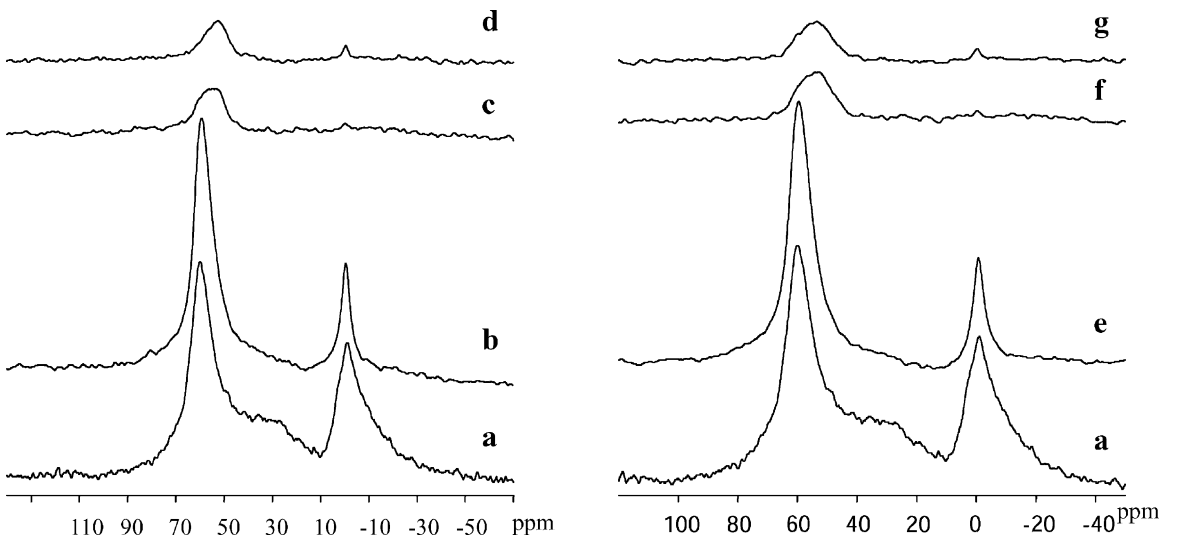

Fig. 4. ^{27}Al MAS NMR spectra of USY after nitric acid (left) and oxalic acid (right) treatments. USY (a), USY(0.25N)HT (b), USY(0.5N)RT (c), USY(0.5N)HT (d); USY(0.1O)HT (e), USY(0.25O)RT (f), USY(0.25O)HT (g).

is removed by the nitric acid, thus resulting in the narrowing of the band at 0 ppm. This conclusion is further checked by MQ MAS NMR in the following section. After the treatment by 0.5N nitric acid at room temperature, the intensity of the 60 ppm peak decreases, with the widening of the line shape and the appearing of a new peak at 52 ppm. Meanwhile, the remaining octahedral aluminum species vanishes (Fig. 4c). When a more rigorous treatment is applied (Fig. 4d), the peak at ca. 60 ppm fades out and only a new signal at ca. 52 ppm can be monitored. The peak at 52 ppm should be attributed to tetrahedral non-framework Al, since the framework structure of the USY breaks down completely after the 0.5N nitric acid treatment under reflux (Fig. 1d). The existence of tetrahedral non-framework Al in dealuminated Y was assumed by Klinowski et al. [44] to explain the lower Si/Al^F ratio determined from the ^{27}Al NMR spectra in comparison with that from the ^{29}Si NMR spectra. Samoson et al. [19] also detected the tetrahedral non-framework Al in hydrothermally treated Y and ZSM-5 zeolites by using 2D NMR spectroscopic techniques. Tetrahedral non-framework Al has been further reported to exist in thermally treated CaA, SrA [45,46] and HMCM-22 zeolites [43].

3.4. ^{27}Al MQ MAS NMR

In this study, ^{27}Al MQ MAS NMR is employed in order to provide unique insight into the dealumination process and for the unambiguous assignment of various Al species in zeolite USY. Figs. 5–8 show the ^{27}Al MQ MAS NMR of the USY, USY(0.25N)HT, USY(0.5N)RT and USY(0.5N)HT, respectively. As shown in the 2D MQ MAS spectra of a series of samples (Figs. 5–8), there is a gradual change in the peak shift and the peak width with the acid leaching conditions. Two distinct bands are observed in the tetrahedral region of the MQ MAS spectrum of USY, i.e. signals A and B. Signal A can be unambiguously assigned to the tetrahedral framework Al (Al^F_{tetra}), and signal B, which appears as a tail to signal A and indicates a much larger quadrupolar coupling due to highly distorted electronic environment, can be attributed to distorted framework tetrahedral Al ($Al^F_{dist.\text{-}tetra}$). The presence of similar Al species has been reported recently by various authors [43,47–50]. Projecting signal B to the F2 dimension gives rise to peaks that span a chemical shift range of $\delta = 20 \sim 40$ and superimpose

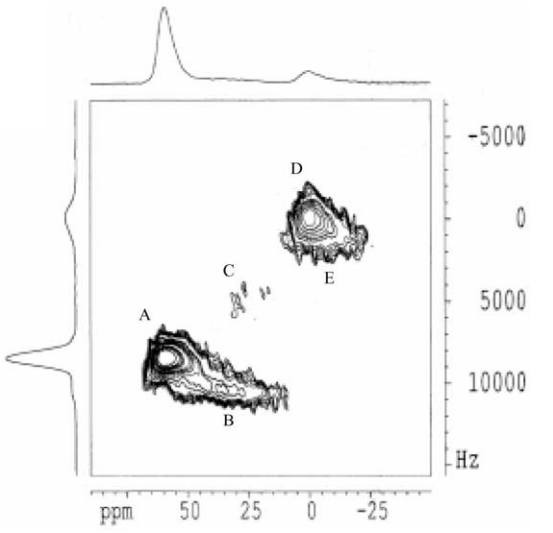

Fig. 5. ^{27}Al 3Q MAS NMR spectrum of parent USY zeolite. Two tetrahedral aluminums ($Al^F_{tetra.}$ (A), $Al^F_{dist.\text{-}tetra.}$ (B)), two octahedral aluminums ($Al^F_{oct.}$ (D), $Al^{NF}_{oct.}$ (E)) and trace of penta-coordinated aluminums ($Al^{NF}_{pent.}$ (C)) are observable.

with that of the five-coordinated non-framework Al ($Al^{NF}_{pent.}$). From these results, it is suggested that the peak at around 30 ppm in the 1D spectra is in fact a superposition of peaks which originate from both

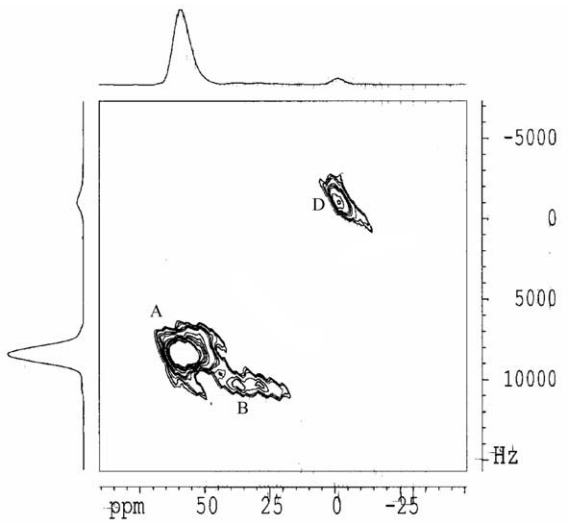

Fig. 6. ^{27}Al 3Q MAS NMR spectrum of USY(0.25N)HT zeolite. Two tetrahedral aluminums ($Al^F_{tetra.}$ (A), $Al^F_{dist.\text{-}tetra.}$ (B)) and one octahedral aluminum ($Al^F_{oct.}$ (D)) are observable.

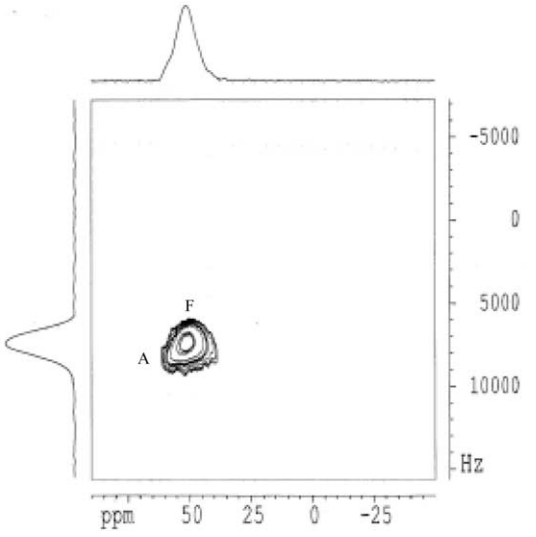

Fig. 7. ^{27}Al 3Q MAS NMR spectrum of USY(0.5N)RT zeolite. Two tetrahedral aluminums ($Al^{F}_{tetra.}$ (A), $Al^{NF}_{tetra.}$ (F)) are observable.

distorted tetrahedral framework Al (signal B in Figs. 5 and 6) and five-coordinated non-framework Al (signal C in Fig. 5). Five-coordinated Al is relatively hard to be observed by MQ MAS NMR due to the different exciting efficiencies of different species, as shown in the recent literature [47,43]. Thus, it is difficult to get

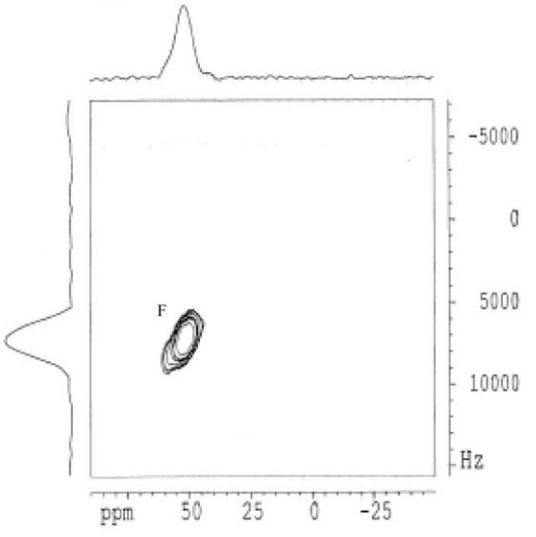

Fig. 8. ^{27}Al 3Q MAS NMR spectrum of USY(0.5N)HT zeolite. One tetrahedral aluminum ($Al^{NF}_{tetra.}$ (F)) is observable.

the exact ratio of these two species just from the MQ MAS NMR. Interestingly, two overlapped signals (one narrow (signal D) and one broad (signal E)) at ca. 0 ppm are discernible in the spectrum of the parent USY. After the 0.25N nitric acid leaching, signal E vanishes and leads to a sharp range at almost an identical position (signal D), suggesting that signal D may be linked with the framework and be attributed to octahedral framework Al ($Al^{F}_{oct.}$) [43,51], while signal E is the octahedral non-framework Al ($Al^{NF}_{oct.}$) species. The regular framework coordination of aluminum in the zeolite framework is tetrahedral. However, there are some evidence that octahedral aluminum ($Al^{F}_{oct.}$) can be present in the framework of a zeolite [43,51–54]. A recent study by Kuehl and Timken [51] on β zeolite has illustrated the detection of a distinct octahedral framework Al^{F} species and a non-framework species. They concluded that the higher the hydrothermal treatment temperature, the smaller the amount of octahedral Al^{F}, and the larger the amount of octahedral Al^{NF} formed. These framework-bound octahedral Al, which were postulated by Wang et al. [55] as intermediate Al species in the hydrolysis process of the framework Al, can be transformed into a tetrahedral coordination by means of ammonia adsorption [43,54,56]. Van Bokhoven et al. [57] also showed that at least two different types of octahedral aluminum exist in β zeolite after a more severe heat treatment. The survival of this signal even after 0.25N nitric acid treatment under reflux proves indirectly that signal D (Fig. 6) should link partly to the zeolite framework. Compared with the octahedral non-framework Al species, octahedral framework Al is more resistant to acid agents.

For the USY zeolite leached by 0.25N nitric acid, the signals due to the five-coordinated Al^{NF} and octahedral Al^{NF} disappeared, and there remain the tetrahedral Al^{F}, the distorted tetrahedral Al^{F}, and the octahedral Al^{F} in its MQ MAS NMR spectrum (Fig. 6). From this point, non-framework Al can be readily removed by acid leaching as expected. After a 0.5N nitric acid treatment at room temperature (Fig. 7), $Al^{F}_{dist.\text{-}tetra.}$ and $Al^{F}_{oct.}$ species were removed, showing that a rigorous treatment can further hydrolyze the remaining Al–O bonds of these species and extract them from the zeolite framework. Meanwhile, a new signal F appears and becomes the dominant peak, with signal A as its shoulder. Signal F is also in the tetrahedral

region, and its projection to F2 dimension results in a chemical shift at 52 ppm. Since most of its framework structure has been collapsed, as indicated by the XRD study, it is reasonable to assign it to tetrahedral non-framework Al ($Al^{NF}_{tetra.}$), as discussed previously in the ^{27}Al MAS NMR. At the same time, the signal corresponding to the tetrahedral framework Al species (signal A) disappears (Fig. 8) when all framework Al are extracted. It has been revealed by Long et al. [58] that when a high temperature steam dealumination treatment is applied, the framework tetrahedral aluminum of HZSM-5 will transform into the non-framework aluminum species that resonances at a similar chemical shift in ^{27}Al MAS NMR. These authors attributed it to the non-framework tetrahedral aluminum species that retains its Si–O–Al links. We believe that a similar reason accounts for the present observation: when a harsh treatment is applied, these framework species, i.e. $Al^{F}_{tetra.}$, $Al^{F}_{dist.\text{-}tetra.}$, etc. will be transformed into the non-framework tetrahedral aluminum species.

From the results presented previously, it can be concluded that dealumination treatment of the USY zeolite by acid leaching can differentiate various coordinations of the Al species. Under mild dealumination conditions, (e.g. concentration <0.25N), the octahedral non-framework Al ($Al^{NF}_{oct.}$) and five-coordinated Al ($Al^{NF}_{pent.}$) are removed at first. At the same time, some of the distorted tetrahedral framework Al ($Al^{F}_{dist.\text{-}tetra.}$) are removed, with a further breaking of its remaining Al–O bonds. Upon intermediate dealumination treatment, the framework Al both in octahedral ($Al^{F}_{oct.}$) and tetrahedral ($Al^{F}_{tetra.}$ and $Al^{F}_{dist.\text{-}tetra.}$) coordinations can be extracted, resulted in the formation of tetrahedral non-framework Al ($Al^{NF}_{tetra.}$) and the collapse of most framework. After severe treatment, however, there remains only the non-framework Al ($Al^{NF}_{tetra.}$) relating to amorphous silica–alumina. Non-framework Al species exhibit not only octahedral and pentahedral but also tetrahedral coordination depending on the dealumination procedures used.

3.5. ^{1}H MAS NMR

High-resolution ^{1}H MAS NMR as a powerful method has been applied frequently to the characterization of the local environment of protons in zeolites. The ^{1}H MAS NMR spectra with different features of the present samples are shown in Fig. 9, and the results after a quantitative deconvolution of the corresponding spectra are plotted simultaneously. The proton distribution is summarized in Table 1. The spectrum of the USY contains signals at 1.6, 2.6, 3.6 and 4.6 ppm, indicating the complexity of the hydroxyl groups. The line at 1.6 ppm, which is the most intense signal in the spectra of acid treated samples, is assigned to non-acidic hydroxyl groups (silanols), and the resonances at about 3.6 and 4.6 ppm, which constitute the maxima in the spectrum of USY, are attributed to SiOHAl groups (Brønsted acid sites) in supercages and sodalite cages, respectively. The signal at 2.6 ppm is due to hydroxyl groups bonded to the non-framework Al [59–61]. As shown in Table 1, 10% of the hydroxyl groups are silanol groups, while the concentration of non-framework Al–OH amounts to 29%.

After the removal of the non-framework Al ($Al^{NF}_{oct.}$ and $Al^{NF}_{pent.}$) and part of the distorted framework tetrahedral Al ($Al^{F}_{dist.\text{-}tetra.}$) by means of a 0.25N nitric acid treatment, the intensity of the line at 2.6 ppm decreases and that of the line at 1.6 ppm increases sharply due to the formation of some additional silanol groups (Fig. 9b). At this stage, the silanol concentration doubles and amounts to 26%. It deserves to be pointed out that the resonance position of Brønsted acid sites in the supercage shifts 0.2 ppm to the low-field. Since the acid strength can be measured

Table 1
The amount of hydroxyls species of different samples[a]

Hydroxyl species	Concentration (%)			
	USY	USY(0.25N)HT	USY(0.5N)RT	USY(0.5N)HT
Si–OH	10.2	26.1	44.5	51.3
Al–OH	28.9	22.6	30.9	34.8

[a] Determined by ^{1}H MAS NMR, the rest are Brønsted acid sites.

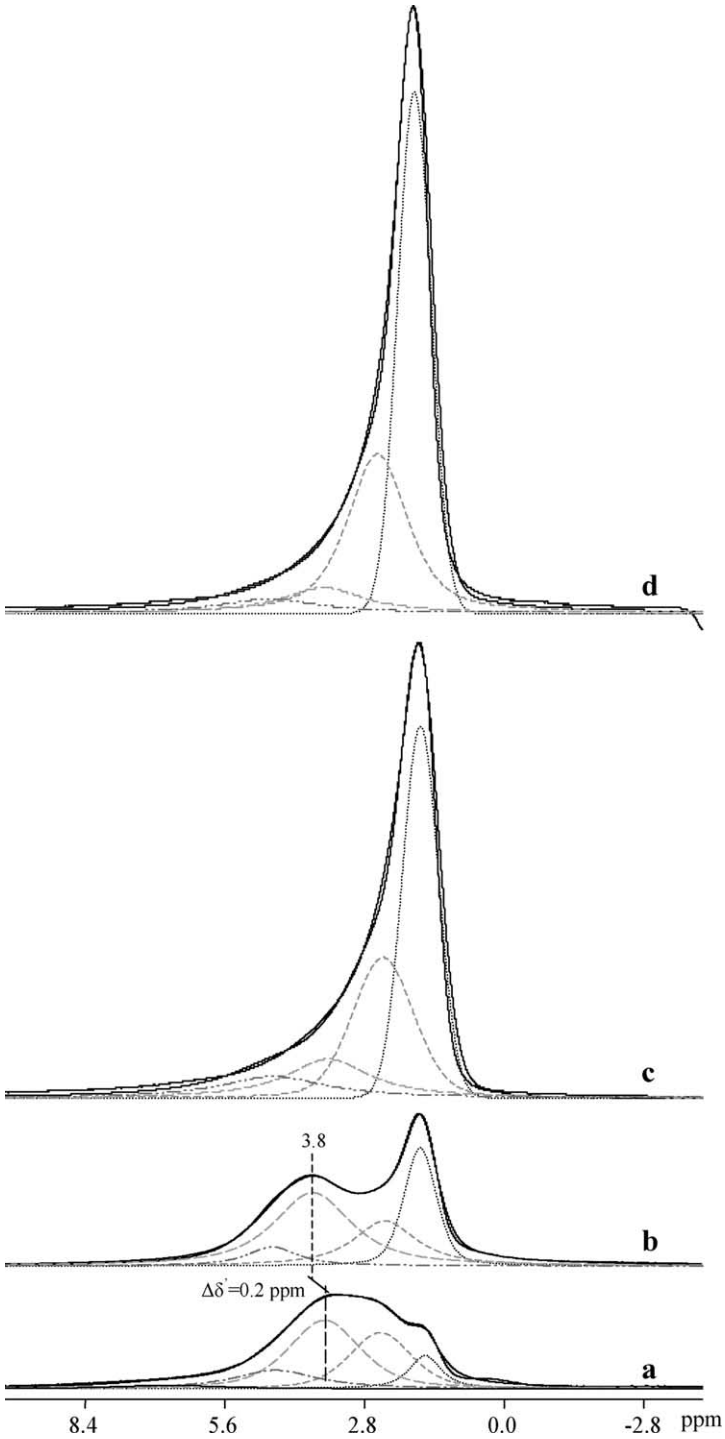

Fig. 9. ^{1}H MAS NMR and their deconvoluted spectra of USY after various treatments. USY (a), USY(0.25N)HT (b), USY(0.5N)RT (c), and USY(0.5N)HT (d).

by the ^{1}H NMR chemical shift [61], this fact reveals that the acid strength of the USY(0.25N)RT may become stronger than that of its parent USY zeolite. Generally, the less the framework aluminum acidic sites a unit cell of a zeolite possesses, the stronger the acidity of the zeolite [62,63]. Theoretical models developed to explain the relationship between acidity and framework composition suggest that, as the initial framework aluminum starts to decrease, the fraction of the "isolated" aluminum atoms increases, resulting in an increase in the acid strength of the active sites [64]. In the present study, some of the framework tetrahedral Al are indeed removed from the zeolite and the removed Al are most likely to be in a distorted tetrahedral geometry, which is apparent from the ^{27}Al NMR experiment. At the same time, all five-coordinated non-framework Al are removed from the pores of the zeolite (as indicated in the ^{27}Al NMR experiments). The five-coordinated non-framework Al may interact with a portion of the remaining structural Al and, thus reduce their acid strength [65]. Both the decrease in the amount of distorted tetrahedrally-coordinated Al and the removal of the five-coordinated Al are suggested to account for the 0.2 ppm shift of the Brønsted acid, which could be interpreted as a leaching-induced increase in the Brønsted acidity. The line at 2.4 ppm is due to the Al–OH species attached to the zeolite framework (framework-related Al–OH, as shown in Fig. 6, $Al^{F}_{oct.}$). These species result from a partial hydrolysis of the framework Al–O bonds due to the interaction of water with the Brønsted acid sites in the zeolite [54]. These framework-bound octahedral Al, which were postulated by Wang et al. [55] as intermediate Al species in the hydrolysis process of the framework Al, can be transformed into a tetrahedral coordination by means of ammonia adsorption [43,54,56]. About 22% of the hydroxyl groups are framework-bound Al–OH species. These results are also consistent with the ^{29}Si CP/MAS NMR, ^{27}Al MAS and MQ MAS experiments discussed previously.

With further treatment (Fig. 9c and d), the signals due to the Brønsted acid sites and Al–OH groups decrease dramatically, while the line at 1.6 ppm increases remarkably and becomes the maximum peak. This is not difficult to imagine: the expelling of one aluminum atom from its tetrahedral position will lead to the formation of four silanol groups (so-called silanol nest). Thus, in the present situation, with most of the aluminum removed from the framework, a great number of silanol groups are formed, which agrees well with a selective enhancement of peaks at −103 and −93 ppm in the corresponding ^{29}Si CP/MAS NMR profiles.

3.6. Relationship between Al sites and n-dodecane cracking activity

The subject of this reaction is to investigate whether and to what extent the different kinds of Al species of USY are able to catalyze the cracking of hydrocarbons. Table 2 lists the products distribution and the

Table 2
Results of *n*-dodecane cracking over USY zeolites

Catalyst	Parent USY	USY(025N)HT	USY(0.5N)RT	USY(0.5N)HT
Product distribution (wt.%)				
Propylene	12.15	11.3	**15.4**	**13.6**
Propane	3.25	3.84	4.37	4.0
iso-Butane	**15.92**	**18.74**	8.56	8.85
iso-Butene	8.1	6.3	**14.76**	**13.88**
n-Butane	4.1	4.3	4.52	4.4
iso-Pentane	**15.6**	**18.1**	6.97	7.1
tran-2-Butene	3.16	2.7	3.91	3.5
tert-Pentane	4.5	3.9	5.5	4.98
2-Methyl-pentane	7.25	7.5	3.1	3.96
3-Methyl-pentane	4.1	4.3	1.8	2.0
2-Methyl-2-butene	4.6	3.2	8.4	7.7
Conversion (%)	45.1	61.57	6.21	9.2

Temperature = 673 K; WHSV = 12 h^{-1}; TOS = 3 min.

n-dodecane conversion at 673 K after 3 min reaction. The data in Table 2 show that *n*-dodecane conversion is different depending on the leaching method used for dealumination. Meanwhile, the primary product selectivities for all the four samples were different. *iso*-Butane and -pentane were the dominant products for parent USY and USY(0.25N)HT samples (as indicated by bold numbers in Table 2). Upon further dealumination, the selectivities for propylene and *iso*-butene increased and became dominant products for USY(0.5N)RT and USY(0.5N)HT samples (as indicated by bold numbers in Table 2).

The large differences in conversion between parent USY and acid-dealuminated USY can be attributed to the different Al sites distribution (type and amount) and, consequently, different reaction mechanisms that prevail. Compared with severe acid-dealuminated USY (USY(0.5N)RT and USY(0.5N)HT), there are large amount of framework tetrahedral Al species in the parent USY and USY(0.25N)HT zeolites, which gives the large amount of Brønsted acid sites and, thus results in the higher *n*-dodecane conversion. At the same time, 0.25N nitric acid leaching results in the appearance of strong acid sites as indicated by ^{1}H MAS NMR. The leaching-induced increase in Brønsted acid strength of USY accounts for the high catalytic activity. Although the USY(0.5N)RT and USY(0.5N)HT samples have little or undetectable framework tetrahedral Al species, there are large amount of non-framework tetrahedral Al species. Peter and Wu [66] observed an active site characterized by a ^{27}Al MAS NMR shift of about 53 ppm after a severe steam dealumination at 830 °C. This species is associated with strong acidity with the Lewis acid character. It is well known that mono-molecular cracking involves secondary reactions, especially further reactions of hexene, pentene and other large alkenes, which contribute to the formation of light alkenes (propylene and *iso*-butene) [67]. The increased non-framework tetrahedral Al species with the significant Lewis acid character [66] favor the secondary reactions, which consequently lead to higher selectivity to propylene and *iso*-butene.

These results suggest that the kinetics of cracking is sensitive to any possible differences in Al sites distributions among these catalysts. The different selectivities implied that different reaction mechanisms for cracking were operative over the four USY samples.

4. Conclusion

Modification of the aluminum distribution of the USY zeolite was carried out by the acids (nitric and oxalic) leaching under various conditions. It is evidenced that the removal of different aluminum species can be controlled by the type and the concentration of the acid and the temperature employed. Depending on the process of acid treatment employed, the removal of non-framework aluminum is followed by that of framework aluminum and, eventually, a collapse of the zeolite framework is observed. Al are extracted at a higher rate by oxalic acid, even at low concentrations. If harsher conditions are applied, a more severe dealumination resulted.

There are five aluminum species in the parent USY zeolite: octahedral aluminum species within and outside the zeolite framework ($Al^{F}_{oct.}$ and $Al^{NF}_{oct.}$), tetrahedral framework Al ($Al^{F}_{tetra.}$), distorted tetrahedral Al ($Al^{F}_{dist.\text{-}tetra.}$) and five-coordinated non-framework Al ($Al^{NF}_{pent.}$). Leaching with 0.25N nitric acid removes mainly those non-framework species, while a further hydrolysis of the remaining Al–O bonds of $Al^{F}_{dist.\text{-}tetra.}$ and $Al^{F}_{oct.}$ is realized under harsher conditions (higher acid concentration or higher treating temperature). For a more rigorous condition, even the tetrahedral framework aluminum is removed from the lattice, leading to the formation of a great number of silanol groups and tetrahedral non-framework aluminum species.

A leaching-induced increase in the Brønsted acidity of USY was observed by ^{1}H MAS NMR spectroscopy, and it is due to the removal of the nearest lattice aluminum species which produces isolated aluminum atoms and the removal of the five-coordinated non-framework aluminum that interacted with the structural aluminum.

The conversion and selectivity for cracking of *n*-dodecane were measured and compared. With the progress of dealumination, the catalytic activity increased at the beginning of the process, reached a maximum, and then decreased. The increase in selectivities to alkenes (propylene and *iso*-butene) was due to the appearance of non-framework tetrahedral Al species resulting from the severe dealumination of USY. The different distribution of Al species in these samples accounted for the different catalytic performance.

Acknowledgements

We are grateful to the supports of the National Natural Science Foundation of China and the Ministry of Science and Technology of China. We thank Dr. R. Fu (NHMFL, Tallahassee) for his kind help regarding the MQ MAS NMR experiments.

References

[1] H. Stach, U. Lohse, H. Thamm, W. Schirmer, Zeolites 6 (1986) 74.
[2] A. Gola, B. Rebours, E. Milazzo, J. Lynch, E. Benazzi, S. Lacombe, L. Delevoye, C. Fernandez, Microporous Mesoporous Mater. 40 (2000) 73–83.
[3] J.M. Cruz, A. Corma, V. Fornes, Appl. Catal. 50 (1989) 287.
[4] F. Lonyi, J.H. Lunsford, J. Catal. 136 (1992) 566.
[5] L. Kubelkova, V. Seidl, J. Novakova, S. Bednarova, P. Jiru, J. Chem. Soc., Faraday Trans. 1 (80) (1984) 1367.
[6] M.W. Anderson, J. Klinowski, Zeolites 6 (1986) 455.
[7] S.T. Sie, Stud. Surf. Sci. Catal. 85 (1994) 587.
[8] M. Trombetta, G. Busca, L. Storaro, M. Lenarda, M. Casagrande, A. Zambon, Phys. Chem. Chem. Phys. 2 (2000) 3529.
[9] B. Li, X. Xu, J. Su, H. Pan, Prep.-Am. Chem. Soc., Div. Pet. Chem. 41 (1996) 369.
[10] S.W. Addidion, S. Cartlidge, D.A. Harding, G. Mcekhiney, Appl. Catal. 45 (1988) 307.
[11] R.M. Lago, W.O. Haag, R.J. Mikovski, D.H. Olson, S.D. Bellring, K.D. Schmitt, G.T. Kerr, New Dev. Zeolite Sci. Technol. 28 (1986) 677.
[12] R.A. Beyerlein, C. Choi-Feng, J.B. Hall, B.J. Hggins, G.J. Ray, Top. Catal. 4 (1997) 27.
[13] J. Rocha, J. Klinowski, J. Chem. Soc., Chem. Commun. (1991) 1121.
[14] X. Yang, R.E. Truitt, Zeolites 16 (1996) 249.
[15] X. Yang, J. Phys. Chem. 99 (1995) 1276.
[16] A.W. Peters, C.C. Wu, Catal. Lett. 30 (1995) 171.
[17] D. Freude, E. Brunner, H. Pfeifer, D. Prager, H.G. Jerschkewitz, U. Lohse, G. Oehlmann, Chem. Phys. Lett. 139 (1987) 325.
[18] L. Kellberg, M. Linsten, H. Jakobsen, J. Chem. Phys. Lett. 182 (1991) 120.
[19] A. Samoson, E. Lippmaa, G. Engelhardt, U. Lohse, H.G. Jerschkewitz, Chem. Phys. Lett. 134 (1987) 589.
[20] G.J. Ray, B.L. Meyers, C.L. Marshall, Zeolites 7 (1987) 307.
[21] G. Garralon, A. Corma, V. Fornes, Zeolites 9 (1989) 84.
[22] L. Kellberg, M. Linsten, H.J. Jakobsen, Chem. Phys. Lett. 182 (1991) 120.
[23] J. Sanz, V. Fornes, A. Corma, J. Chem. Soc., Faraday Trans. I 84 (1988) 313.
[24] S.M.C. Menezes, V.L. Camorim, Y.L. Lam, R.A.S. San Gil, A. Bailly, J.P. Amoureux, Appl. Catal. Part A: Gen. 207 (2001) 367.
[25] G. Engelhardt, D. Michel, High-Resolution Solid-State NMR of Silicates and Zeolites, Wiley, New York, 1987 (Chapter V. 3.4).
[26] J.P. Gilson, G.C. Edwards, A.W. Peters, K. Rajagopalan, R.F. Wormsbecher, T.G. Roberie, M.P. Shatlock, J. Chem. Soc., Chem. Commun. (1987) 91.
[27] D.C. Koningsverger, J.T. Miller, Stud. Surf. Sci. Catal. 101 (1996) 841.
[28] A. Pines, M.G. Gibby, J.S. Waugh, J. Chem. Phys. 56 (1972) 1776.
[29] W. Zhang, D. Ma, X. Liu, X. Liu, X. Bao, J. Chem. Soc., Chem. Commun. (1999) 1091.
[30] D. Ma, Y. Shu, W. Zhang, W. Han, Y. Xu, X. Bao, Angew. Chem. Int. Ed. 39 (2000) 2928.
[31] A. Samoson, E. Lippmaa, A. Pines, Mol. Phys. 65 (1988) 1013.
[32] A. Llor, J. Virlet, Chem. Phys. Lett. 152 (1988) 248.
[33] L. Frydman, J.S. Harwood, J. Am. Chem. Soc. 117 (1995) 5367.
[34] Z. Gan, J. Am. Chem. Soc. 122 (2000) 3242.
[35] A. Medek, J.S. Harwood, L. Frydman, J. Am. Chem. Soc. 117 (1995) 12779.
[36] A.P.M. Kentgens, D. Iuga, M. Kalwei, H. Koller, J. Am. Chem. Soc. 123 (2001) 2925.
[37] R.R. Ernst, G. Bodenhausen, A. Wokaun, Principles of Nuclear Magnetic Resonance in One and Two Dimensions, Clarendon Press, Oxford, 1987.
[38] J.P. Amoureux, C. Fernandez, S. Steuernagel, J. Magn. Reson. A 123(9) (1996) 116.
[39] W.A. Dietz, J. Gas Chromat. 5 (1967) 68.
[40] E. Bottari, L. Ciavatta, Gazz. Chim. Ital. 98 (1968) 1004.
[41] E. Lippmaa, M. Mägi, A. Samoson, M. Tarmak, G. Engelhardt, J. Am. Chem. Soc. 103 (1981) 4992.
[42] J. Dwyer, F.R. Fitoh, F. Machado, G. Qin, S.M. Smyth, J.C. Vickman, J. Chem. Soc., Chem. Commun. (1981) 422.
[43] D. Ma, X. Han, S. Xie, X. Bao, H. Hu, S.C.F. Au-Yeung, Chem. -A Eur. J. 8 (2002) 162.
[44] J. Klinowski, C.A. Fyfe, G.C. Gobbi, J. Chem. Soc., Faraday Trans. I 81 (1985) 3003.
[45] D.R. Corbin, R.D. Farlee, G.D. Stucky, Inorg. Chem. 23 (1984) 2920.
[46] D. Freude, J. Haase, H. Pfeifer, D. Prager, G. Scheler, Chem. Phys. Lett. 114 (1985) 143.
[47] C.A. Fyfe, J.L. Bretherton, L.Y. Lam, Chem. Commun. (2000) 1575.
[48] T.-H. Chen, B.H. Wouters, P.J. Grobet, Eur. J. Inorg. Chem. (2000) 281.
[49] J.A. Van Bokhoven, A.L. Roest, D.C. Koningsberger, J.T. Miller, G.H. Nachtegaal, A.P.M. Kentgen, J. Phys. Chem. B 104 (2000) 6743.
[50] A. Gola, B. Rebours, E. Milazzo, J. Lynch, E. Benazzi, S. Lacombe, L. Delevoye, C. Fernandez, Microporous Mesoporous Mater. 40 (2000) 78.
[51] G.H. Kuehl, H.C. Timken, Microporous Mesoporous Mater. 35 (2000) 521.
[52] L.C. de Ménorval, W. Buckermann, F. Figueras, F. Fajula, J. Phys. Chem. 100 (1996) 465.

[53] G.L. Woolery, G.H. Kuehl, H.C. Timken, A.W. Chester, J.C. Vartuli, Zeolites 19 (1997) 288.
[54] B.H. Wouters, T.H. Chen, P.J. Grobet, J. Am. Chem. Soc. 120 (1998) 11419.
[55] Q.L. Wang, G. Giannetto, M. Torealba, G. Perot, C. Kappenstein, M. Guisnet, J. Catal. 130 (1991) 459.
[56] B.H. Wouters, T.H. Chen, P.J. Grobet, J. Phys. Chem. B 105 (2001) 1135.
[57] J.A. Van Bokhoven, D.C. Koningsberger, P. Kunkeler, H. van Bekkum, A.P.M. Kentgens, J. Am. Chem. Soc. 122 (2000) 12842.
[58] Y.-C. Long, M.-Y. Jin, Y.-J. Sun, T.-L. Wu, L.-P. Wang, L. Fei, J. Chem. Soc., Faraday Trans. 92 (1996) 1647.
[59] M. Hunger, Catal. Rev. Sci. Eng. 39 (1997) 345.
[60] E. Brunner, J. Mol. Struct. 355 (1995) 61.
[61] M. Hunger, D. Freude, H. Pfeifer, Catal. Today 3 (1988) 507.
[62] P.J. Kooyman, P. van der Waal, H. van Bekkum, Zeolites 18 (1997) 50.
[63] R. Carvajal, P.-J. Chu, J.H. Lunsford, J. Catal. 125 (1990) 123.
[64] D. Barthomeuf, Mater. Chem. Phys. 17 (1987) 49.
[65] J.T. Miller, P.D. Hopkins, B.L. Meyers, G.J. Ray, R.T. Roginski, G.W. Zajac, N.H. Rosenbaum, J. Catal. 138 (1992) 115.
[66] A.W. Peter, C.C. Wu, Catal. Lett. 30 (1995) 171.
[67] S.M. Babitz, B.A. Williams, J.T. Miller, R.Q. Snurr, W.O. Haag, H.H. Kung, Appl. Catal. 179 (1999) 71.